

Supporting Information

Precise design and in-situ synthesis of hollow $\text{Co}_9\text{S}_8@\text{CoNi-LDH}$ heterostructure for high performance supercapacitors

Jiachao Zhou,^a Yingchao Wang,^a Linli Chen,^a Wenna Zhao^{*,b} and Lei Han^{*,a}

^a State Key Laboratory Base of Novel Functional Materials and Preparation Science, School of Materials Science and Chemical Engineering, Ningbo University, Ningbo, Zhejiang 315211, China.

^b School of Biological and Chemical Engineering, Ningbotech University, Ningbo, Zhejiang 315100, China

*E-mail: hanlei@nbu.edu.cn; wz Zhao@nit.zju.edu.cn

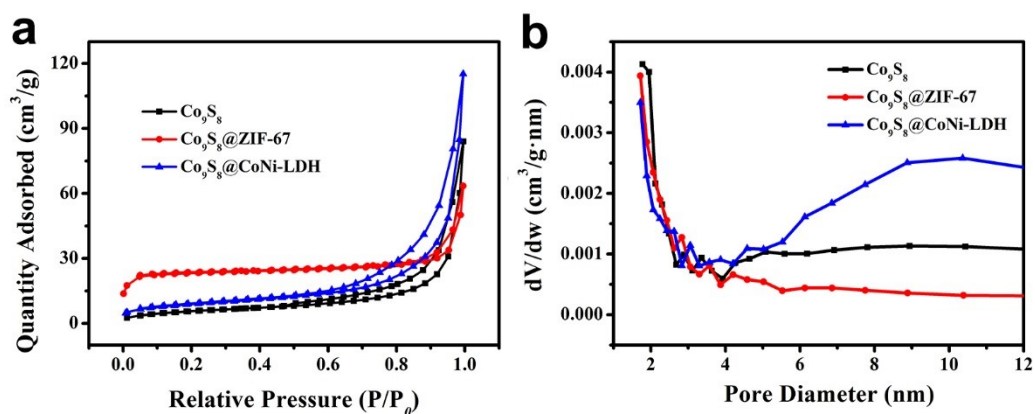


Fig. S1 (a) N_2 adsorption-desorption isotherms and (b) pore-size distribution of Co_9S_8 , $\text{Co}_9\text{S}_8@\text{ZIF-67}$ and $\text{Co}_9\text{S}_8@\text{CoNi-LDH}$.

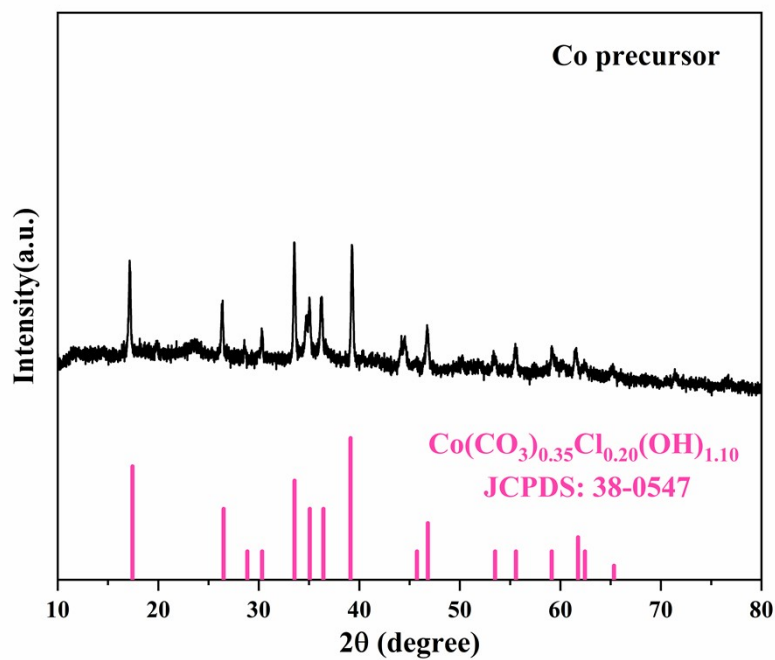


Fig. S2 XRD pattern of Co precursor.

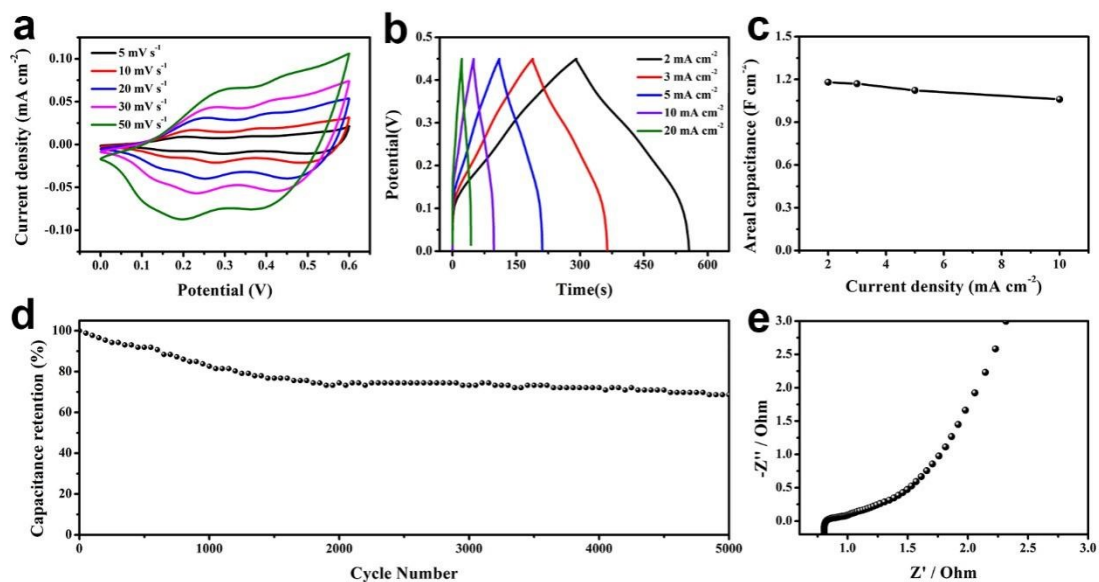


Fig. S3 The electrochemical properties of CoCH/NF. (a) CV curves at scan rates of 5-50 mV s^{-1} ; (b) GCD curves at current density of 2-20 mA cm^{-2} ; (c) The specific capacitance at current densities of 1-10 mA cm^{-2} ; (d) The cycling capacity after 5000 cycles, (e) Nyquist plots of ESI.

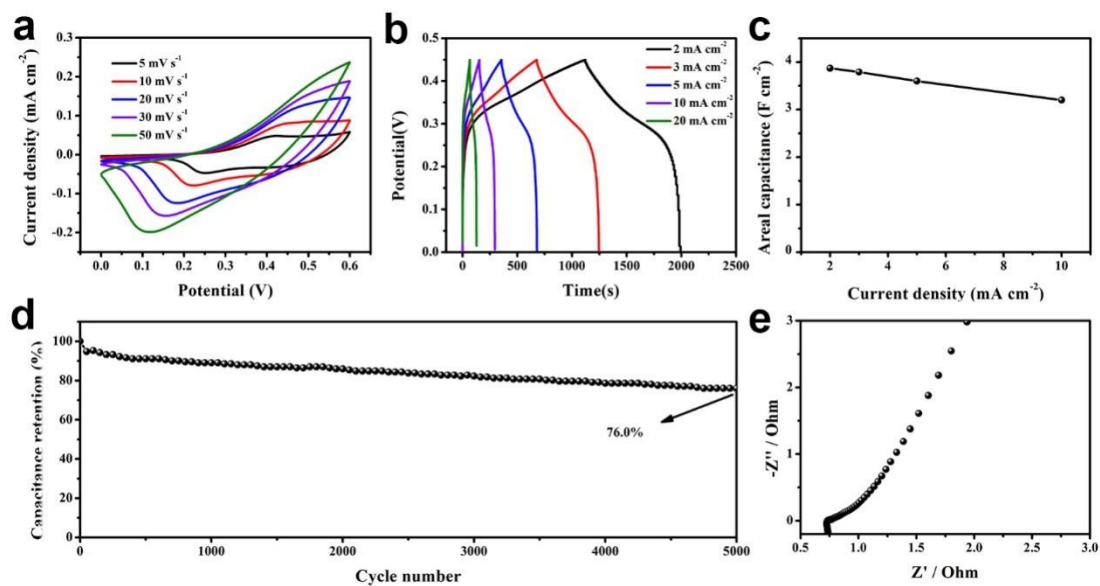


Fig. S4 The electrochemical properties of $\text{Co}_9\text{S}_8/\text{NF}$. (a) CV curves at scan rates of 5-50 mV s^{-1} ; (b) GCD curves at current density of 2-20 mA cm^{-2} ; (c) The specific capacitance at current densities of 1-10 mA cm^{-2} ; (d) The cycling capacity after 5000 cycles, (e) Nyquist plots of ESI.

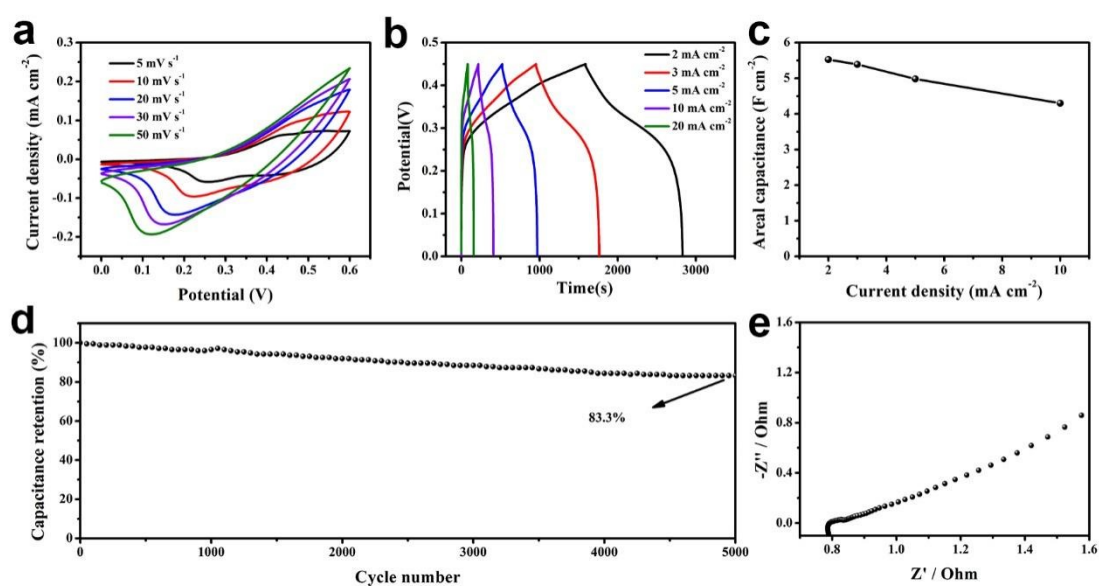


Fig. S5 The electrochemical properties of $\text{Co}_9\text{S}_8@\text{ZIF-67}/\text{NF}$. (a) CV curves at scan rates of 5-50 mV s^{-1} ; (b) GCD curves at current density of 2-20 mA cm^{-2} ; (c) The specific capacitance at current densities of 1-10 mA cm^{-2} ; (d) The cycling capacity after 5000 cycles, (e) Nyquist plots of ESI.

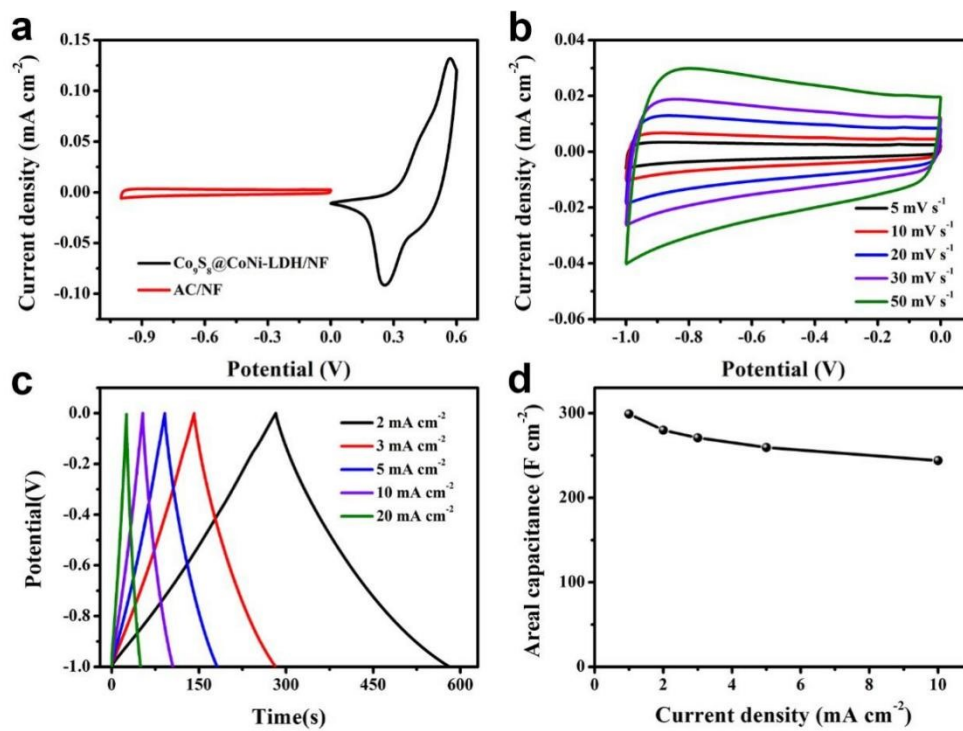


Fig. S6 (a) The CV curves of AC and $\text{Co}_9\text{S}_8@\text{CoNi-LDH/NF}$; (b) The CV curves of the AC at scan rates of $5\text{-}50 \text{ mV s}^{-1}$; (c) The GCD curves of AC at current density of $2\text{-}20 \text{ mA cm}^{-2}$; (d) The specific capacity of AC at current densities of $1\text{-}10 \text{ mA cm}^{-2}$.

Table S1 The capacitance comparison of other CoNi-LDH based electrode materials

Electrode material	Specific capacitance	Cycle performance	Ref.
CNTs/Ni Co LDH	1628 F g ⁻¹ at 1 A g ⁻¹	78.073% after 5000 cycles	S1
H-NiCo LDH@ACC	1377mC/cm ² at 1mA/cm ²	70% after 10000 cycles	S2
CoNi-LDH	986.3 F g ⁻¹ at 1 A g ⁻¹	92.3% after 10000 cycles	S3
CNMnL-m	1644 F g ⁻¹ at 1 A g ⁻¹	94.2% after 5000 cycles	S4
Ni _x Co _{1-x} LDH/AC	947 F g ⁻¹ at 1 A g ⁻¹	80% after 5000 cycles	S5
CoNi LDH@Co ₃ O ₄ @CC	1021.7 F g ⁻¹ at 10 A g ⁻¹	Not mentioned	S6
Ni/Co-LDH	1652 F·g ⁻¹ at 1 A·g ⁻¹	99% after 2000 cycles	S7
NiCoAl-LDH/NF	5691.25 mF cm ⁻² at 1 mA cm ⁻²	73.5% after 3000 cycles	S8
4M-P@NiCo LDH	7 F cm ⁻² at 50 mA cm ⁻²	72.5% after 5000 cycles	S9
(Ni,Co)Se ₂ /NiCo-LDH	1224 F g ⁻¹ at 2A·g ⁻¹	89.5% after 3000 cycles	S10
Co ₃ O ₄ @Ni-Co LDH/NF	1069 C g ⁻¹ at 1 A·g ⁻¹	67.9% after 5000 cycles	S11
Co ₉ S ₈ @CoNi-LDH	9.7 F cm ⁻² (2411 F g ⁻¹ , 1085 C g ⁻¹) at 2 mA cm ⁻²	92% after 5000 cycles	This work

References

- S1. M. Huang, Y. Wang, J. Chen, D. He, J. He and Y. Wang, Biomimetic design of Ni Co LDH composites linked by carbon nanotubes with plant conduction tissues characteristic for hybrid supercapacitors, *Electrochim. Acta*, 2021, **381**, 138289.
- S2. X. Xuan, M. Qian, L. Han, L. Wan, Y. Li, T. Lu, L. Pan, Y. Niu and S. Gong, In-situ growth of hollow NiCo layered double hydroxide on carbon substrate for flexible supercapacitor, *Electrochim. Acta*, 2019, **321**, 134710.
- S3. B. Huang, W. Wang, T. Pu, J. Li, J. Zhu, C. Zhao, L. Xie and L. Chen, Two-dimensional porous (Co, Ni)-based monometallic hydroxides and bimetallic layered double hydroxides thin sheets with honeycomb-like nanostructure as positive electrode for high-performance hybrid supercapacitors, *J. Colloid Interface Sci.*, 2018, **532**, 630-640.
- S4. W. Quan, Y. Xu, Y. Wang, S. Meng, D. Jiang and M. Chen, Hierarchically structured

Co₃O₄@glucose-modified LDH architectures for high-performance supercapacitors, *Appl. Surf. Sci.*, 2019, **488**, 639-647.

S5. T. Chen, L. Luo, X. Wu, Y. Zhou, W. Yan, M. Fan and W. Zhao, Three dimensional hierarchical porous nickel cobalt layered double hydroxides (LDHs) and nitrogen doped activated biocarbon composites for high-performance asymmetric supercapacitor, *J. Alloys Compd.*, 2021, **859**, 158318.

S6. D. Wang, L. Tian, D. Li, Y. Xu and Q. Wei, Rational design of Co–Ni layered double hydroxides electrodeposited on Co₃O₄ nanoneedles derived from 2D metal-organic frameworks for high-performance asymmetric supercapacitors, *J. Electroanal. Chem.*, 2020, **873**, 114377.

S7. Z. Xiao, Y. Mei, S. Yuan, H. Mei, B. Xu, Y. Bao, L. Fan, W. Kang, F. Dai, R. Wang, L. Wang, S. Hu, D. Sun and H. C. Zhou, Controlled Hydrolysis of Metal-Organic Frameworks: Hierarchical Ni/Co-Layered Double Hydroxide Microspheres for High-Performance Supercapacitors, *ACS Nano*, 2019, **13**, 7024-7030.

S8. P. Li, Y. Jiao, S. Yao, L. Wang and G. Chen, Dual role of nickel foam in NiCoAl-LDH ensuring high-performance for asymmetric supercapacitors, *New J. Chem.*, 2019, **43**, 3139-3145.

S9. G. Wang, Z. Jin and W. Zhang, A phosphatized NiCo LDH 1D dendritic electrode for high energy asymmetric supercapacitors, *Dalton Trans.*, 2019, **48**, 14853-14863.

S10. X. Li, H. Wu, C. Guan, A. M. Elshahawy, Y. Dong, S. J. Pennycook and J. Wang, (Ni,Co)Se₂/NiCo-LDH Core/Shell Structural Electrode with the Cactus-Like (Ni,Co)Se₂ Core for Asymmetric Supercapacitors, *Small*, 2019, **15**, 1803895.

S11. Y. Zhang, Y. Wang, J. Zhu, X. Zhang and W. Cai, Regulating the core/shell electric structure of Co₃O₄@Ni-Co layered double hydroxide on Ni foam through electrodeposition for a quasi-solid-state supercapacitor, *Nanotechnology*, 2021, **32**, 345702.